13

Electrochemical Aspects in Biomedical Alloy Characterization: Electrochemical Impedance Spectroscopy

Carlos Valero Vidal and Anna Igual Muñoz
Universidad Politécnica de Valencia
Spain

1. Introduction

Metals and alloys are widely used as biomedical materials and are essential for orthopaedic implants, bone fixations, artificial joints, external fixations... since they can substitute for the function of hard tissues in orthopaedic. In particular, toughness, elasticity, rigidity, and electrical conductivity are important properties for metallic materials used in medical devices. Because the most important property of biomaterials is safety and biocompatibility, corrosion-resistant materials such as stainless steel, cobalt-chromium-molybdenum alloys and titanium alloys are commonly employed. However, there is still a significant concern associated with biomedical alloys related to the production of metal particles and ions (Fleury et al., 2006; Okazaki & Gotoh, 2005) which can lead to cellular toxicity (Germain et al., 2003; Catelas et al., 2001; Horowitz et al., 1998), metal hypersensitivity (Granchi et al., 2005; Hallab et al., 2000), and chromosomal changes (Massè et al., 2003).

Corrosion of orthopedic biomaterials is a complex multifactorial phenomenon that depends on geometric, metallurgical, mechanical and physico-chemical parameters, thus a firm understanding of these factors and their interactions is required in order to comprehend how and why implant materials fail (corrode, degrade). Electrochemical measurements are powerful in situ methods that allow analyzing the interface properties and corrosion behaviour between metal biomaterials (passive oxide film) and the involved body fluids. Within this group of techniques, the Electrochemical Impedance Spectroscopy (EIS) is a useful tool which provides information about the interface, its structure, passive film properties and the reactions taking place on the interface electrolyte/oxide passive film. The impedance spectroscopy is a technique that permits the measurement of uniform corrosion and passive dissolution rates, the elucidation of reaction mechanisms, the characterization of surface films and it is also used for testing coatings or surface modifications.

The aim of the present chapter is to describe the EIS technique and its potentiality in the fundamental understanding of the processes occurring at the metal/human body interface in bio-systems. The chapter will be mainly focused on its application in characterizing CoCrMo biomedical alloys.

2. Corrosion: an electrochemical reaction

The corrosion process is an irreversible chemical or electrochemical reaction occurring at the interface of the material representing the spontaneous dissolution of the metal (M) by its reaction with the environment resulting in the loss of the material or in the dissolving of one of the constituents of the environment into the material (Landolt, 2007). The oxidation of the metal, equation (1), is coupled to the reduction of the oxidizing agent (environment) which takes the electrons from the oxidation reaction. The equations (2) and (3) show the reduction reactions favoured in acidic media, while the equations (4) and (5) take place in neutral or basic media.

$$M \rightarrow M^{+n} + ne^{-} \tag{1}$$

$$2H^{+} + 2e^{-} \rightarrow H_2 \tag{2}$$

$$O_2 + 4H^{+} + 4e^{-} \rightarrow 2H_2O \tag{3}$$

$$O_2 + 2H_2O + 4e^{-} \rightarrow 4OH^{-} \tag{4}$$

$$2H_2O + 2e^{-} \rightarrow H_2 + 2OH^{-} \tag{5}$$

Fig. 1 shows a scheme of the reaction steps (anodic and cathodic) occurring at the biomaterial surface during the corrosion process in liquid environments.

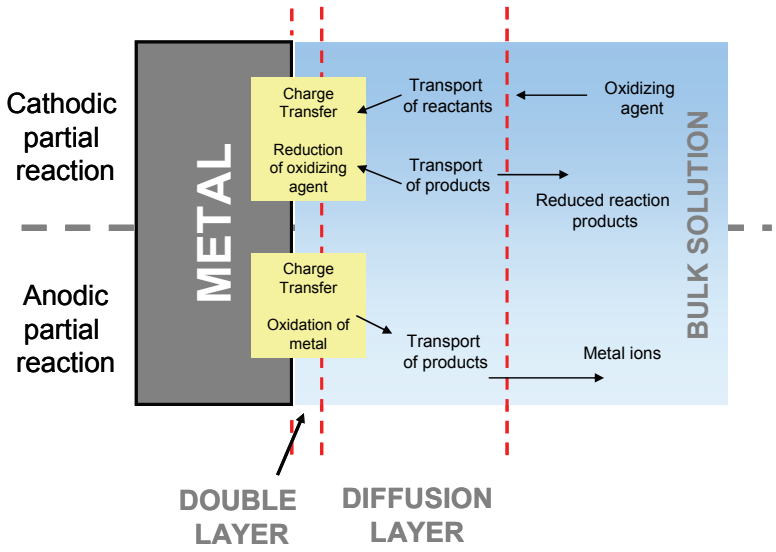

Fig. 1. Reaction steps during the corrosion of a metal in liquid environments (Landolt, 2007).

In a bio-system involving metallic biomaterials several corrosion phenomena can take place: active dissolution, passivation, passive dissolution, transpassive dissolution, localized corrosion and adsorption.

The **passivity** of metals consists in the formation of a thin oxide layer on their surface which protects the metal from its environment. Thus, the biomaterials are self-protected by the spontaneous formation of this thin oxide film being the kinetic factor that controls the corrosion rate in biological aqueous solutions. Therefore, the biocompatibility of these biomaterials is closely related to the stability of this oxide layer. The passive film plays two roles in limiting both the anodic and cathodic reactions, serving as a physical barrier for cations (ions positive charged) and anions (ions negative charged) transported to the metal surface as well as an electronic barrier for electrons.
On the other hand, the metals free of oxide film are in their **active state**. The dissolution of these metallic materials is denominated **active dissolution** and involves a charge transfer at the metal-electrolyte interface. The ions generated are dissolved into the solution in form of hydrated or complexed species according to equation (1). However, **passive dissolution** takes place when passive metals are dissolved. In this case, the cations are also generated in the interface metal-oxide film by a charge transfer reaction and the ions migrate across the passive film-electrolyte interface. Equation (6) shows the formation of the oxide film as a consequence of the cation (M^{+n}) migration towards the outer surface and the anion (O^{-2}) migration in the opposite direction while the equation (7) represents the passive dissolution where the cations are dissolved from the passive film into the solutions. The overall reaction (equations (6) and (7)) is equivalent to equation (1).

$$M + \frac{n}{2} H_2O \rightarrow MO_{n/2} + nH^+ + ne^- \tag{6}$$

$$MO_{n/2} + nH^+ \rightarrow M^{+n} + \frac{n}{2} H_2O \tag{7}$$

Transpassive dissolution: occurs when the protecting passive film is oxidized to species with higher solubility (i.e. Cr^{+6}, Co^{+6}) (Marcus & Oudar, 1995). It can occur below the potential for oxygen formation (uniform transpassive dissolution by film oxidation) or when oxygen evolution is observed (high-rate transpassive dissolution). Dissolution at transpassive potentials is relevant to corrosion in strongly oxidizing media.
An important type of corrosion is the **localized corrosion** in which an intensive attack takes place in small local sites at a much higher rate than the rest of the surface (which is corroding at a much lower rate). The localized corrosion is associated with other mechanical process (such as stress, fatigue and erosion) and others forms of chemical attack. The main form of localized corrosion in passive alloys (i.e. stainless steel) is the **pitting corrosion**; the metal is removed preferentially from vulnerable areas on the surface. The pitting corrosion is a local dissolution leading to the formation of cavities in passive metals or alloys that are exposed to environments with aggressive ions (i.e. chlorides) (Szklarska-Smialowska, 1986; Bi et al., 2009).
Other common phenomenon in biological systems is **adsorption** of certain species presents in the body fluid (i.e. proteins) onto the surface of metallic materials. The adsorption is established between the adsorbed species and the surface due to weak forces or the Van der Waals and it can modify the passive dissolution rate of the biomaterials among others.

3. Fundamentals of the electrochemical impedance spectroscopy

The Electrochemical Impedance Spectroscopy (EIS) is a relatively modern technique widely extended in several scientific fields. The EIS consists on a non-destructive technique when

working under equilibrium conditions (free corrosion potential or open circuit potential), particularly sensible to small changes in the system that allows to characterize material properties and electrochemical systems even in low conductive media.
The impedance method consists in measuring the response of an electrode to a sinusoidal potential modulation of small amplitude (typically 5-10 mV) at different frequencies. The alternative current (ac) modulation is superimposed either onto an applied anodic potential or cathodic potential or onto the corrosion potential (Scully et al., 2003).

3.1 Electrode response to a sinusoidal perturbation of the potential

An excitation sinusoidal signal $E(t)$ is superimposed onto the steady-state potential of an electrode, expressed as a function of time (t):

$$E(t) = E_0 \cdot \cos(\omega f) \tag{8}$$

where E_0 is the amplitude (in volts), ω is the radial frequency (in radians per second) defined also as $\omega=2\pi f$ and f is the frequency expressed in Hertz (Hz). In order to maintain a linear response of the electrode the modulation amplitude must not exceed 10mV.
The sinusoidal introduction of the perturbation of potential on the system induces a sinusoidal current $I(t)$. The response signal $I(t)$ is shifted in phase and has different amplitude.

$$I(t) = I_0 \cdot \cos(\omega f - \varphi) \tag{9}$$

where I_0 is the amplitude (in amperes) and φ is the phase (in degrees).
The **Electrochemical Impedance** (Z) is defined as the relation between the applied potential and the resulting intensity. The impedance expresion is function of the magnitude (Z_0) and the phase shift (φ). The ratio of the amplitudes of the applied signal and the response signal on the one hand and the phase shift between both signals on the other determines the impedance.

$$Z = \frac{E(t)}{I(t)} = \frac{E_0 \cdot \cos(\omega f)}{I_0 \cdot \cos(\omega f - \varphi)} = Z_0 \frac{\cos(\omega t)}{\cos(\omega t - \varphi)} \tag{10}$$

Using Euler's relationship (equation (11)) it is possible to represent these functions in the complex plane.

$$\exp(i\theta) = \cos\theta + isen\theta \tag{11}$$

where i^2=-1 is the imaginary number and θ is the angle.
The sinusoidal perturbation of the potential and the current response are represented therefore by two vectors in the complex plane. Thus, the impedance Z is represented by a vector sum of the real and the imaginary part (equation (13)) characterized by the modulus Z_0 and the phase shift φ.

$$Z = \frac{E_0 \exp(j\varpi t)}{I_0 \exp(j\varpi t - j\varphi)} = Z_0 \exp(j\varphi) = Z_0(\cos\varphi + jsen\varphi) \tag{12}$$

$$Z = Z_{\mathrm{Re}} + j\, Z_{\mathrm{Im}} \tag{13}$$

The modulus (equation (14)) and the phase shift (equation (15)) can be calculated using Pythagoras' theorem and the adequate trigonometric relations:

$$|Z| = \sqrt{Z_{\mathrm{Re}}^2 + Z_{\mathrm{Im}}^2} \tag{14}$$

$$\theta = \arctan\left(\frac{Z_{\mathrm{Im}}}{Z_{\mathrm{Re}}}\right) \tag{15}$$

Two graphical representations of the impedance spectrum are possible. If the impedance Z is represented in the complex plane, where the real part is plotted on the x-axis and the imaginary part on the y-axis of a chart for different frequencies, the graphic is called **Nyquist diagram** (Fig. 2(a)).
The impedance can also be represented displaying the modulus $|Z|$ (in logarithmic scale) and the phase shift φ (both on the y-axis) as a function of the logarithmic of the frequency f. This presentation method is the **Bode plot** (Fig. 2(b)).

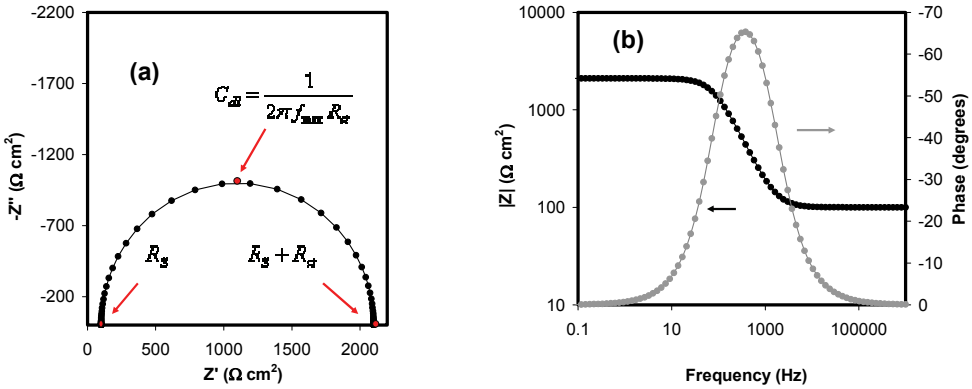

Fig. 2. (a) Nyquist diagram and (b) Bode plot of impedance data for a simple equivalent circuit (Randless circuit with solution resistance (R_s) of 100Ωcm², double layer capacitance (C_{dl}) of 1·10⁻⁶Fcm⁻² and charge transfer resistance (R_{ct}) of 2000Ωcm²).

3.2 Interpretation of the impedance results

The interpretation of the impedance spectra requires the selection of an electric model that suitably fits the experimental data to a combination of electrical elements, Table 1. Thus, according to the selected model and its properties it is possible to obtain information about the electrochemical mechanisms and properties of the system. Common electrical elements and their corresponding meaning are described as follows:

- Resistance (R): describes some charge transfer across certain interface (i.e. metal/electrolyte).
- Capacitance (C): is characteristic to charge structures (double layers) considering these layers as parallel plate condenser.
- Inductance (L): is associated with adsorption-desorption process occurring in the formation of layers (passive film).

- Warburg (W): it represents linear diffusion under semi-infinite conditions. This also assumes the diffusion layer to possess an infinite thickness. The Warburg impedance is defined through an admittance Y_0, and a diffusion parameter B.

Table 1 summarizes the real and imaginary part of the impedance expression of the commonly used electrical elements.

The simplest equivalent circuit used for fitting the experimental results is represented in the Fig. 3. In this case, the theoretical transference function is represented by means of parallel combination of the resistance R_{ct} (charge transfer resistance) and the capacitance C_{dl} (double layer capacitance related to the interactions in the electrode/electrolyte interface) both in series with the resistance R_s (electrolyte resistance).

Element	Impedance
Resistance	R
Capacitance	$-\frac{i}{\omega C}$
Inductor	$i\omega L$
Warburg (infinite)	$-\frac{1}{Y_0\sqrt{i\omega}}$
Warburg (finite)	$\frac{\tanh\left(B\sqrt{i\omega}\right)}{\left(Y_0\sqrt{i\omega}\right)}$

Table 1. Impedance expression of the electrical elements.

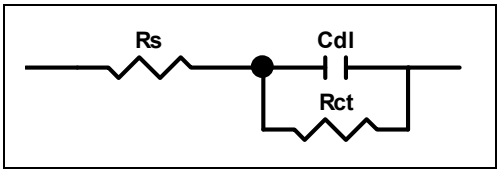

Fig. 3. Equivalent Electric Circuit (Randless) of the electrode-electrolyte interface.

The impedance value of the system represented in Fig. 3 is shown in equation (16):

$$Z(\omega) = R_S + \left(\frac{1}{\frac{1}{R_{ct}} + i\,\omega C_{dl}} \right) \tag{16}$$

The impedance spectrum obtained for the Randless Circuit is represented in Fig. 2. This spectrum shows, in the higher frequency region, that $log|Z|$ tends to a constant value with a phase shift close to 0^o when the frequency increases. This is a resistive behaviour and the values of the impedance correspond to R_S.

In the medium-lower frequencies range a linear relationship between $log|Z|$ and $log\ f$ is observed. For an ideal capacitive behaviour the slop is approximately -1. Generally, the non-

ideal systems present certain modification from an ideal capacitance behavior (lower value of the slope and lower phase angles). A constant phase angle element (CPE) is introduced to replace the capacitance and to describe the non-ideal behaviour which can be due to different physical phenomenon such as surface heterogeneity resulting from surface roughness, impurities, dislocations or grain boundaries. CPE is defined as:

$$Z(\omega) = Z_0(i\omega)^{-n} \tag{17}$$

where Z_0 is the CPE constant and n is the CPE exponent. Depending on n, CPE can represent resistance (n=0, Z_0=R), a capacitance (n=1, Z_0=C) or a Warburg impedance (n=0.5, Z_0=W). For $0.5<n<1$ the CPE describes a distribution of dielectric relaxation times in the frequency space.

The value of the capacitance is a useful parameter since it could be related to the film thickness according to the following expression (Helsen & Breme, 1998):

$$C = \varepsilon \cdot \varepsilon_0 \cdot \frac{A}{d} \tag{18}$$

where ε denotes the relative dielectric constant of the layer, ε_0 is the permittivity of the vacuum (8.85×10^{-14} Fcm^{-1}), A the active area (in cm^2) and d the film thickness (in cm).

In general, the usual guidelines for the selection of the best-fit EEC are (i) a minimum number of circuit elements employed to describe the electrochemical system, (ii) the Chi-squared value (X^2) should be suitable low ($X^2 \leq 10^{-4}$) and (iii) the errors associated with each element must be up to 5% (Metikos, 2006).

3.3 Instrumentation

A conventional three-electrode cell configuration is commonly employed for carrying out the EIS experiments. A potential (V) is applied between the working electrode (WE, i.e. biomaterial) and the reference electrode (RE, i.e. Ag/AgCl electrode) and the current density (I) flowing through the working electrode and the counter electrode (CE, i.e. platinum) is measured.

The basic electronic instrumentation that allows to obtain the impedance spectra in electrochemical systems consists on a generator-analyzer of functions denominated Frequency Response Analyzer (FRA) or "lock-in amplifier". The FRA can analyze and apply sinusoidal signals in a widespread frequencies range to the potentiostat with fast response and sensibility.

A potentiostat applies a sinusoidal signal (equation (8)) to the working electrode in the electrochemical cell. The latter is often built into a two-channel transfer function analyzer, thus permitting simultaneously measurement of the potential and the current. The system responds with a signal (equation (9)) that differs from the equation (8) by its phase and amplitude. The response of the electrode, measured by the analyzer, determines the impedance Z response of the electrochemical system and the phase shift corresponding to each frequency.

3.4 Experimental considerations for biomaterials

Biological systems are specific corrosion media which requires several experimental considerations in order to obtain significant data from EIS measurements:

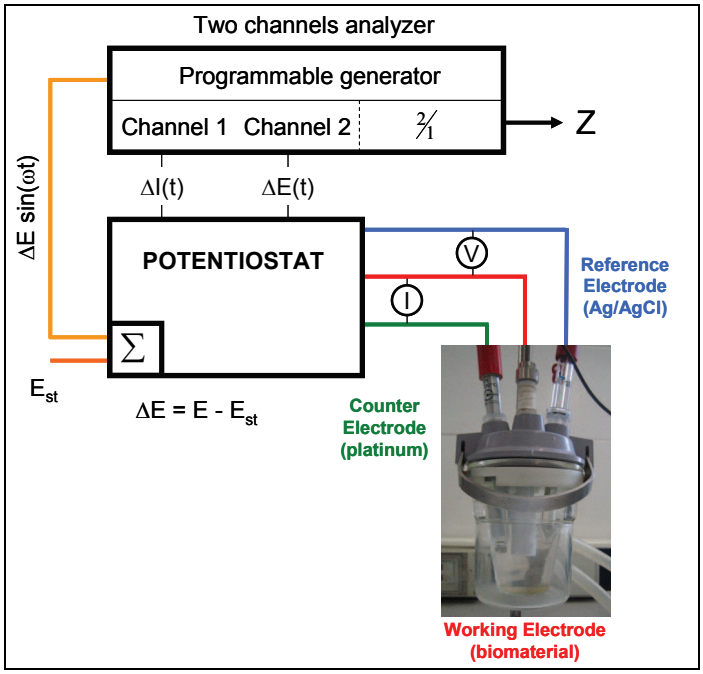

Fig. 4. Experimental set up for impedance measurements using a transfer function analyser under potentiostatic control (a sinusoidal of weak amplitude $\Delta E=E-E_{st}$ is superimposed onto the steady state potential E_{st} of an electrode).

1. The properties of the biomaterials and the biological environments may strongly change depending on the electrochemical conditions. Selection of very low frequencies in the impedance sweep requires longer experimental times and might conduct changes in the electrode surface, altering the steady-state conditions needed for the adequate impedance measurements. Thus, it is important to adapt the final frequency of the sweep to the system since it can introduce error in the impedance measurements obtained at the lowest frequencies (Hodgson et al., 2004).
2. The adsorption of organic compounds on the electrode surfaces may affect the impedance response; i.e. the adsorption of proteins in the reference electrode may cause errors in the potential measurements.
3. The biological solutions are highly susceptible to be contaminated by external agents (such as acids and metallic ions). For this reason, it is important the cleaning of the instrumentation to carry out the experimental tests. Furthermore, the use of sterilized materials is advisable when accurate results are desirables.

4. CoCrMo biomedical alloys

Biomaterials for medical devices and prostheses are implanted into the human body to replace, repair or restore the function of the tissues or bones. Metals are more suitable for load-bearing applications compared with ceramic or polymeric materials because they combine high mechanical strength, high fracture toughness and good processability.

However, the failure of the implants and their revision at relative short times is commonly required. For example, it has been documented higher rate of failure ranking from 30% to 56% in patients under 40 years of age after 10-12 years when conventional hip arthroplasty was performed (Ebied & Journeaux et al., 2002). In particular, about 10% of the metal-on-metal (MoM) total hip replacements (THR) implanted since 1988 had to be replaced in the last years (Wolner et al, 2006). Nevertheless, the MoM replacements are required over other type of materials (i.e. UHMWPE implants) since they improve the osteolisis problems among others (Tipper et al., 2005). Therefore, there is a need to use metallic materials as implant devices (due their good benefits) but it is necessary to reduce the failure and revision times.

Within the group of metallic biomaterials for implants, cobalt-chromium-molybdenum alloys (CoCrMo) are widely used in the last years. These alloys are characterized for their highly biocompatibility and corrosion resistance and they are a good alternative for orthopaedics and dental prosthesis. There are basically two types of Co-Cr alloys in clinical practice; CoCrMo alloy (F75-87) used in as-cast pieces and CoNiCrMo alloy (F562-84) adapted for forged pieces at high temperatures. The latter is mainly used in those cases where mechanical loads are required. On the other hand, there are some other Co-Cr alloys with iron and tungsten addition but they are not so commonly used in implant devices: CoCrWNi (F90-87) and CoNiCrMoWFe (F563-88).

4.1 General electrochemical behaviour of the CoCrMo biomedical alloy

The high biocompatibility of the CoCrMo is related to the spontaneous formation of an oxide film that protects the metal from the surrounding environment (body fluid). It is well known that the properties of this oxide film control the chemical and mechanical properties of the biomaterial and therefore, its durability into the human body. The physico-chemical properties of the passive film also control the corrosion behaviour of the materials, the interaction with tissues and the electrolyte and thus the degree of the material biocompatibility. The properties of the film may change depending on the external conditions (i.e. temperature, potential…) but usually present similar composition due to the stability of that passive film.

The composition of the passive film of CoCrMo alloys presents high content in Cr (mainly Cr(III) and smaller amount of $Cr(OH)_3$) with a minor contribution of Co and Mo oxides (Milosev & Strehblow, 2003; Hodgson et al., 2004; Igual & Mischler, 2007; Valero et al., 2010). A direct relation between the thickness of the passive film and the applied potential (increasing around 1nm/V in the passive domain) was observed by Milosev and Strehblow (2003). Hanawa et al. (2001) studied by X-ray photoelectron spectroscopy (XPS) the surface oxide film formed on CoCrMo in quasi-biological environments and determined that Cr and Mo were distributed at the inner layer of the film while the Co was dissolved from the film, reaching a thickness of 2.5-2.9 nm.

The exact chemistry of the passive layer is highly dependent on the chemical composition of the electrolyte (Igual & Mischler, 2007; Valero & Igual, 2008). Therefore, special care has to be taken when formulating the simulated body fluids in order to obtain electrochemical results for clinical application.

From this point of view, the main components present in the body fluids are salts (NaCl, KCl, $CaCl_2$), organic molecules (proteins) and inorganic species (phosphates). The general composition of the human biological fluids (plasma or serum and synovial fluid) is shown

in Table 2. Fluid properties and composition can readily change as a result of disease, aging and drug ingestion (Black & Hastings, 1998).
At this moment, there is not a general consensus in the scientific community about the best "simulated body fluid" to be used for characterizing metallic biomedical alloys. Further research the influence of the solution chemistry on the corrosion mechanisms is required to solve this problem (to avoid this uncertainty).

Compound	Plasma (serum)	Synovial fluid
Bicarbonate	25-30 mM	-
Calcium	2.12-2.72 mM	1.2-2.4 mM
Cloride	100-108 mM	87-138 mM
Phosphorous (total)	2.87-4.81 mM	-
Potassium	3.5-4.7 mM	3.5-4.5 mM
Sodium	134-143 mM	133-139 mM
Amino acids	20-51 mg/mL	-
Glucosa	650-966 mg/mL	-
Uric acid	30.5-70.7 mg/mL	39 mg/mL
Water	930-955 mg/mL	960-988 mg/mL
Albumin	37.6-54.9 mg/mL	6-10 mg/mL
IgG	6.4-13.5 mg/mL	1.47-4.62 mg/mL
Fibrinogen	2-4 mg/mL	-

Table 2. General chemical composition of the human biological (Black & Hastings, 1998).

4.1.1 Passive dissolution of CoCrMo alloys

The main corrosion mechanism of CoCrMo alloys in the body fluids is passive dissolution. In vitro (Germain et al., 2003; Okazaki & Gotoh, 2005) and in vivo (Massè et al., 2003; Dumbleton & Manley, 2005) tests confirm the metal release from the CoCrMo alloys through that corrosion mechanism. Different variety of phenomena as a consequence of metal ion release takes place into the human body such as transportation, metabolism, accumulation in organs, allergy and carcinoma (Hanawa, 2004). These effects can be generally harmful for human health, mainly in the case of the CoCrMo where the alloying elements Cr and Co generate high risk of carcinogenicity. Although the definitive effects of these metal ions have not been determined, toxicity and metall alergy are the most significant concerns. For example, it has been demostrated that Cr^{3+} and Co^{+2} have a toxicity effect on osteoblasy and induced cell mortality (Fleury et al., 2006).
Therefore, there is still a need of fundamental understanding of the electrochemical behaviour of CoCrMo alloys in order to improve their corrosion resistance and minimize the metal ion releases in the human body.

4.2 Evaluation of the electrochemical behaviour of CoCrMo alloys by EIS

EIS has demonstrated to be a useful tool to analyze the corrosion behaviour of the CoCrMo biomedical alloys as well as to study the modifications of the properties of the passive film depending on several external conditions (i.e. temperature, chemical composition of the electrolyte, potential). It is possible to obtain information about the passive film dissolution (kinetics) and passive film properties (film thickness, passive film dielectric constants, diffusion coefficient of the diffusing species) by EIS.

The CoCrMo alloy spontaneously passivates resulting in the formation of an oxide film in contact with the biological environment (biofilm) according to the scheme represented in Fig. 5. EIS results under passive conditions (Fig. 6(a)) show high values of impedance (around 100KΩcm^2) which can be due to two superposed semicircles (time constants). Those impedance results are good fitted with the EEC proposed in Fig. 6(a), consisting on two R-C groups disposed in series. The physical meaning of the selected EEC is attributed to the resistance oxide (R_{in})/capacitance (C_{in}) in parallel combination across the oxide and to the charge transfer resistance (R_{out})/double layer capacitance (C_{out}) parallel combination. In this case, R_p (polarization resistance of the system) can be calculated as the sum of R_{out} and R_{in} after fitting the experimental results to the EEC.

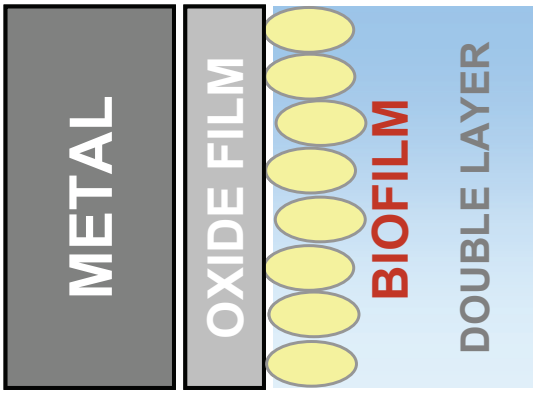

Fig. 5. Scheme of the interface of a metallic surface in contact with biological environments where the metal is covered by an oxide layer, and by an adsorbed organic film ("biofilm").

Because the corrosion mechanisms are highly dependent on the prevailing electrochemical conditions (i.e. applied potential), Fig. 6 shows the EIS spectra obtained at different applied potentials; (a) passive, (b) cathodic and (c) transpassive. Under cathodic conditions (Fig.6(b)) the impedance values at high frequencies are much lower than in the passive domain, because the cathodic reaction is favoured thus reducing passivation. At low frequencies the slope of 45^o in the Nyquist diagram is observed and this feature is characteristic of Warburg-like behaviour. The impedance data are fitted to the Equivalent Circuit presented in Fig. 6(b). The elements of the EEC proposed are R_s (solution resistance), CPE_{out} (constant phase element of the double layer), R_{out} (charge transfer resistance of the outer layer) and W-R (Warburg element) related to the mass transport limitation by diffusion. The high frequencies loop can be attributed to the charge transfer which takes place at the interface. The low frequencies loop represents to the diffusion of dissolved oxygen from the electrolyte to the interface.

The presence of oxidizing agents in the electrolyte may favour the anodic reaction of the passive film and modifies the interface solution-alloy. The impedance spectrum under transpassive conditions (Fig. 6(c)) is characterized by a high frequency capacitance loop related to the charge transfer due to the dissolution of the metal as a result of the anodic applied potential, an inductive loop at medium frequency and a semi-arc obtained at the lowest frequencies which indicates the presence of an inner surface film. The EEC proposed to describe the system is shown in Fig. 6(c). The circuit consists of the following elements:

CPE_{out} represents the capacity of the metal/film/electrolyte interface, R_{out} is the outer layer resistance, RL element (resistance and inductance) is attributed to the relaxation of the corrosion product on the electrode surface, CPE_{in} is the capacitance of the inner oxide layer and the R_{in} the inner oxide layer resistance.

Therefore, EIS technique has been demonstrated to be a useful tool to analyze the corrosion behaviour of CoCrMo alloys as well as to study the modification of the passive film properties depending on the applied potential under potentiostatic conditions.

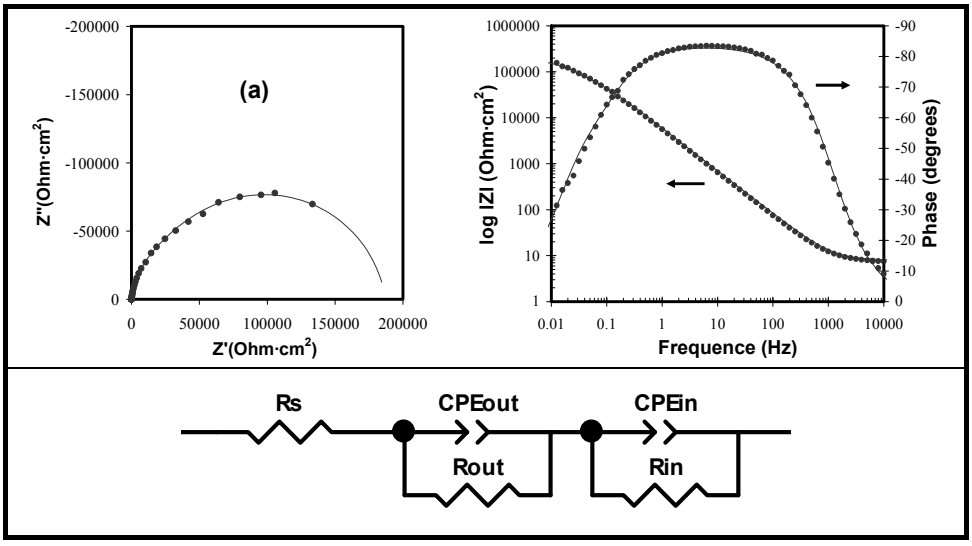

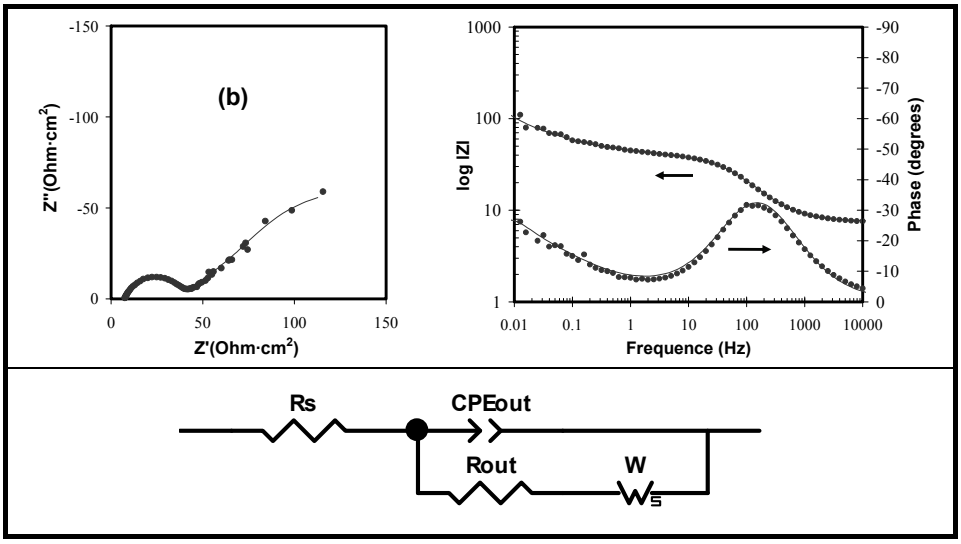

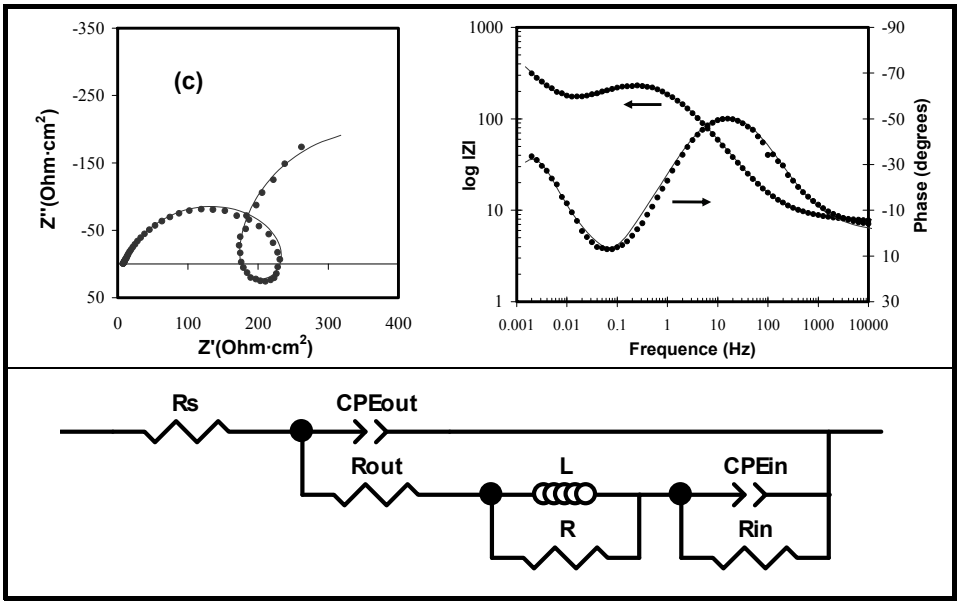

Fig. 6. Nyquist diagrams (left), Bode plots (right) and Equivalent Electrical Circuits (bottom) of a CoCrMo alloy at (a) passive (b) cathodic and (c) transpassive potential in bovine serum solution at 37ºC and pH 7.4.

4.2.1 Influence of temperature

Temperature is an important parameter that can change electrochemical reaction rates. In biological systems, temperature favours the release of metallic ions into the body and it can even change the corrosion mechanisms from that occurring at room temperature (Virtanen et al., 2008). It is necessary to control the temperature when carrying out electrochemical in-vitro tests since certain chemical compounds (i.e. proteins) can modify their behaviour depending on this parameter. For example, some proteins modify their conformational structure with temperature. The Bovine Serum Albumin (BSA), the most common protein in the fluids of human body, is characterized by its globular structure with high tendency to aggregate in macromolecular assemblies, where its three-dimensional structure is composed of three domains, each one formed by six helices and its secondary structure in α-helix. This structure is perfectly defined and stabilized at room temperature however, when the temperature increases, some molecular regions become accessible to new intermolecular interactions, producing soluble aggregates through disulphide and non-covalent bonds (Militello et al., 2003). Temperature can also modify the behaviour of inorganic species, i.e. the precipitation of Ca-phosphates is favoured at higher temperatures and it is hardly observed at room temperature. The precipitation of inorganic species can form a layer covering the biomaterial surface, blocking the mass transport of oxygen and/or of reaction products and/or from the alloy surface reducing the corrosion rate and the ion release. Thus changes in temperature contributes to changes in the corrosion mechanisms.

Impedance spectra of a CoCrMo alloy in form of Nyquist diagrams and Bode plots at different temperatures are shown in Fig. 7(a) and Fig. 7(b) respectively. The main effect of

temperature on the corrosion behaviour of the CoCrMo alloy is the decrease of the R_{ct} values, which is due to the higher passive dissolution rate of the alloy. Temperature also displaces the maximum value of the phase diagrams in the Bode plots towards higher frequencies which is related to a modification of the double layer capacitance.

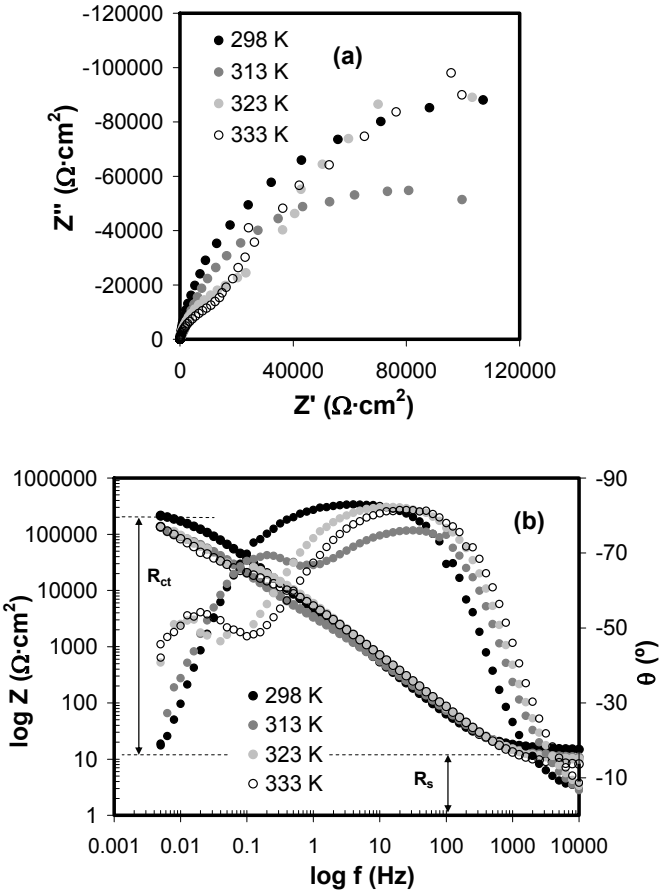

Fig. 7. (a) Nyquist diagrams and (b) Bode plots of a CoCrMo alloy at OCP in NaCl+50 mg/L BSA at different temperatures and pH 7.4 (Valero & Igual, 2010).

The Bode plots (Fig. 7(b)) clearly shows two phase maxima which correspond to two time constants in the electrochemical system. According to the EEC proposed in Fig. 6(a) the experimental impedance data has been fitted to the two RC groups disposed in series and the calculated electrical parameters show that CPE_{in} increases with temperature indicating the diminution of the thickness of the passive film (equation (18)). The decrease of the R_{out} with temperature is related to the denaturation process of the protein.

An important chemical parameter that allows one to correlate the temperature with the rate of the corrosion process taking place in the biomaterial interface is the **activation energy** (*Ea*, $Jmol^{-1}$). This parameter is generally defined as the minimum energy required to start a

chemical reaction or the energy that must be overcome for a chemical reaction to occur. The EIS technique permits to obtain the activation energy of an electrochemical process in a temperature range for a fixed electrolyte composition. The procedure for determining the activation energy from EIS measurements is described as follows:
The Arrhenius equation is represented as:

$$i_{corr} = A \cdot e^{-E_a/RT} \tag{19}$$

where i_{corr} (Acm^{-2}) is the corrosion current density (current flowing under steady-state conditions), T (K) is the temperature, R ($Jmol^{-1}K^{-1}$) is the gas constant and A is a pre-exponential factor.
Corrosion current density (i_{corr}) is related to the R_{ct} through the Stern-Geary equation:

$$i_{corr} = \frac{b_a b_b}{2.303(b_a + b_b)} \cdot \frac{1}{R_{ct}} \tag{20}$$

where b_a and b_c ($V\ decade^{-1}$) are the anodic and cathodic Tafel slopes (obtained from polarization measurements) respectively, and are defined as $b_{a,c}=2.303RT/\alpha_{a,c}F$ (where α is the charger transfer coefficient and F is the Faraday's constant with the value of 96500 C/eq). Applying logarithms to equation (19) and substituting i_{corr} by equation (20) the following expression is obtained:

$$\ln \frac{R_{ct}}{T} = \frac{E_a}{R} \cdot \frac{1}{T} + \text{constant} \tag{21}$$

From the plot of $\ln(R_{ct}/T)$ against $1/T$ it is possible to obtain a straight line which slope gives one the Ea of the corrosion process.
Fig. 8 shows an example of the influence of BSA on the Ea of a CoCrMo alloy. R_{ct} values were extracted from EIS tests carried out at different temperature and BSA concentrations (Valero et al., 2010)

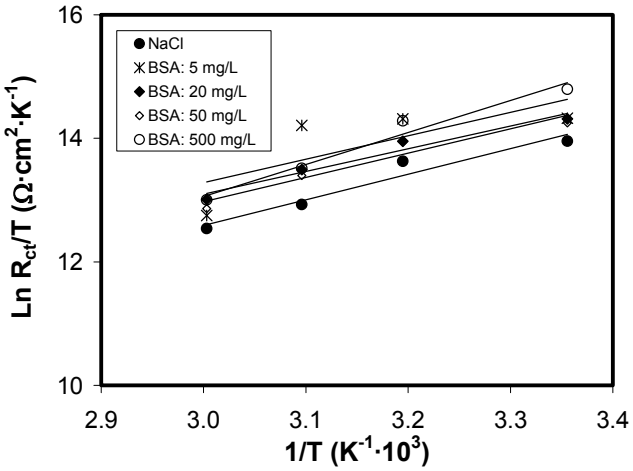

Fig. 8. Effect of temperature on the charge transfer resistance of CoCrMo alloy in 0.14M NaCl and different BSA additions, Arrhenius plot (Valero et al., 2010).

The increase of BSA concentration caused a decrease in the corrosion activation energy which means that the adsorption of BSA molecules onto the CoCrMo surface occurred by charge transfer mechanism, favouring the corrosion reaction occurring on metal surface.

4.2.2 Influence of the chemical composition of the simulated body fluid

The body fluids are considered high corrosive solutions due the presence of several aggressive compounds such a chloride ions and complex species (proteins) at relative high temperature (37ºC).

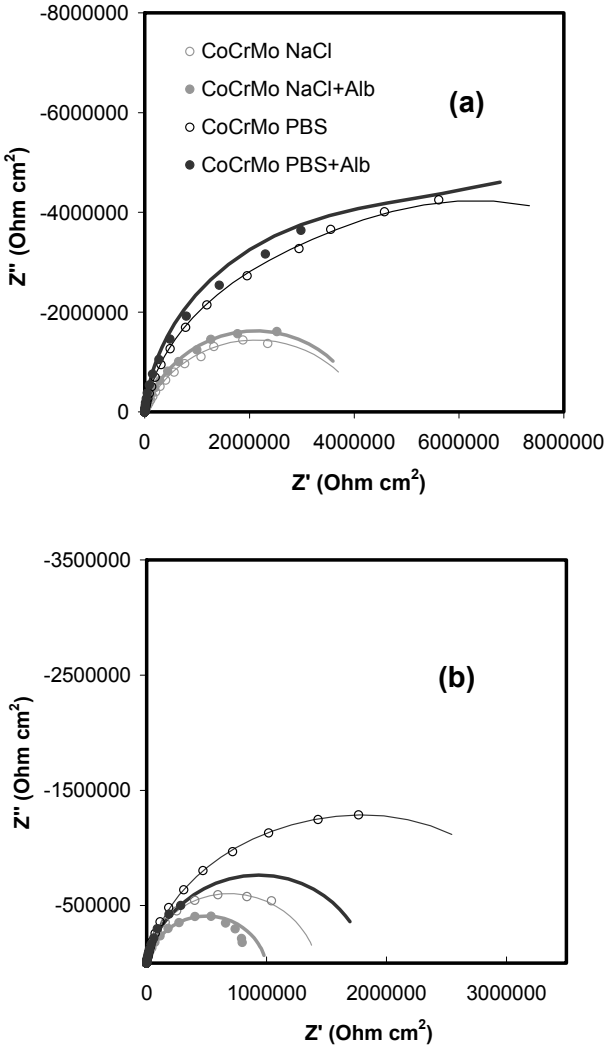

Fig. 9. Nyquist diagram of CoCrMo in different solutions at (a) passive potential and (b) OCP, pH 7.4 and 37ºC (Igual & Mischler, 2007).

EIS can be employed to investigate changes in the interface passive film/electrolyte on CoCrMo depending on the chemical composition of the electrolyte. Fig. 9 shows the Nyquist Diagrams obtained at an applied passive potential (Fig. 9(a)) and at OCP (Fig. 9(b)) in different simulated body fluids. Under potentiostatic conditions a well-defined electrochemistry can be achieved and therefore the effect of solution chemistry on CoCrMo corrosion behaviour can be studied.
The Nyquist diagrams are different depending on the solution chemistry. Phosphates (PBS) increased the corrosion resistance of the alloy under both electrochemical conditions (higher diameter of the Nyquist semicircle) while the effect of the BSA varies depending on the applied potential. This behaviour can be explained by the competitive adsoption of phosphates ions and BSA molecules on the CoCrMo alloy. The adsorption of phosphates produces a blocking effect on the passive film and reduces the corrosion rate of the alloy. The adsorption of the BSA can act in different ways: it limits the adsorption of phosphates (accelerating the corrosion) but can modify the passive film properties and, by acting as cathodic inhibitor, can reduce the corrosion rate. The EIS is a good tool for determine the different actuation of these components.
The EIS results can be fitted to the EEC shown in Fig. 6(a) and it is observed that the solution chemistry does not significantly affect the thickness of the passive film. This conclusion is obtained from the analysis of the values of the resistance R_{in} and capacitance CPE_{in}; all those values slightly change in presence of BSA and PBS. On the contrary, different solution compositions lead to larger effects on the electrical properties of the outer layer (R_{out} and CPE_{out}). These results are in good agreement and well-supported with Surface Analysis (X-Ray Photoelectron Spectroscopy (XPS) and Auger Electron Spectroscopy (AES)) (Igual & Mischler, 2007).
When comparing the impedance results at the different applied potentials, passive potential (Fig.9(a)) and OCP (Fig.9(b)) it is possible to observe that the higher resistance is related to the highest applied potential (applied potential). The effect of both, PBS and BSA depends on the prevailing electrochemical conditions (surface chemistry).

4.2.3 Adsorption of proteins

The study of the adsorption of proteins onto metallic surfaces can be carried out by EIS (Igual & Mischler, 2007; Valero & Igual, 2008; Valero et al.; 2010). There is an increasing interest in the interfacial behaviour of proteins in the metallic components implanted in the human body as a result of problems associated to bacterial growth (Khan et al., 1996; Kanagaraja et al., 1996) and metal dissolution (Hallab et al., 2001; Virtanen et al., 2008). In the field of biomaterials and medical implants, it is widely accepted that one event that significantly influence the biocompatibility and stability of the biomaterial is the nearly instantaneous adsorption of proteins from biological fluids.
Analyzing the theoretical isotherm which better fits the protein behaviour allows one to characterize the protein adsorption mechanisms by means of chemical parameters.
Specially, the adsorption of the BSA onto the CoCrMo surface is described by the Langmuir isotherm:

$$\Gamma = \frac{B_{ADS}\Gamma_{\max}c}{1 + B_{ADS}c} \tag{22}$$

where c (mol cm^{-3}) is the equilibrium concentration of the adsorbate (BSA) in the bulk solution, Γ (mol cm^{-2}) is the amount of protein adsorbed, i.e. surface concentration, Γ_{max} (mol cm^{-2}) is the maximum values of Γ, and the parameter B_{ADS} (cm^3 mol^{-1}) reflects the affinity of the protein molecules towards adsorption sites.
The parameters Γ_{max} and B_{ADS} can be determined by rearranging the equation (22):

$$\frac{c}{\Gamma} = \frac{1}{B_{ADS}\Gamma_{\max}} + \frac{c}{\Gamma_{\max}} \tag{23}$$

A plot of c/Γ versus concentration should yield a straight line with parameters Γ_{max} and B_{ADS} derived from the slope and intercept, respectively. The surface concentration (Γ) of BSA can be correlated with the charge transfer resistance due the protein addition ($R_{ct,c}$), i.e. $1/R_{ct,c} \propto \Gamma$ (proportional). The resistance values can be obtained from the corrected values for the resistance obtained in the protein-free solution ($R_{ct,0}$) in each incremental addition of protein ($R_{ct,i}$) by the expression:

$$R_{ct,c} = R_{ct,i} - R_{ct,0} \tag{24}$$

In the equation (23) the surface concentration (Γ) can be substituted by the resistance values. Thus, the dependence of $c \cdot R_{ct,c}$ versus BSA concentration in the solution it is also linear over the investigated temperature range. This procedure allows obtaining B_{ADS} and Γ_{max} parameters from EIS data (Valero et al., 2010).
The parameter B_{ADS}, which reflects the affinity of the adsorbate molecules toward adsorption sites at a constant temperature, can be presented as:

$$B_{ADS} = \frac{1}{c_{solvent}} \exp\left(\frac{-\Delta G_{ADS}}{RT}\right) \tag{25}$$

where ΔG_{ADS} (J mol^{-1}) is the Gibbs free energy of adsorption, and $c_{solvent}$ is the molar concentration of a solvent, which in this case is the water (c_{H2O} = 55.5 mol dm^{-3}).
Finally, it is possible to determine the enthalpy and the entropy related to the adsorption process from Gibbs free energy:

$$\Delta G_{ADS} = \Delta H_{ADS} - T \cdot \Delta S_{ADS} \tag{26}$$

Fig. 10 shows the ΔG_{ADS} results of the study carried out on the adsorption mechanisms of BSA on a CoCrMo alloy using EIS (Valero et al., 2010) according to the previous procedure. The positive value of ΔH_{ADS} shows that the process is endothermic. The gain in entropy represents the driving force for the adsorption of the protein onto the metallic surface (the term $T\Delta S_{ADS}$ is considerably higher than the enthalpy value). These results reflects that the structure and hence dimensions of the molecule changes when the protein adsorbs onto the metallic surface. The induced structural changes can lead to a considerably entropy gain, which appears to be the driving force for the adsorption of the BSA.

4.2.4 Effect of the microstructure

In order to improve the corrosion and wear resistance of CoCrMo alloys, they are commonly subjected to different thermal treatments (i.e. solution annealing, hot isostatic pressure). Fig. 11 shows examples of the microstructures of an as-cast commercial CoCrMo alloy subjected to three thermal treatments:

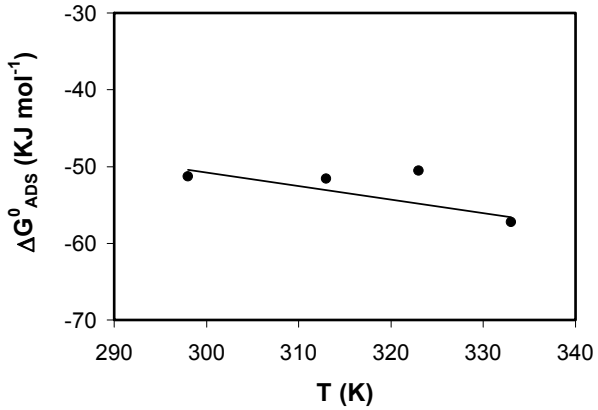

Fig. 10. Dependence of the Gibbs energy of adsorption on the temperature for BSA onto CoCrMo surface in NaCl solution (pH 7.4) by EIS (Valero et al., 2010).

- **Treatment 1**: solution annealing (cyclic thermal treatment) applied after as-cast process. A typical temperature cycle of one solution annealing in CoCrMo biomedical alloy consist of maintaining the alloy at 1119ºC during 240 minutes (in inert atmosphere) and cooling before at 24ºC/min until reaching the temperature of 760ºC. The combination of temperature and time is variable depending on the material and the desirable conditions.
- **Treatment 2**: a solution annealing + hot isostatic pressing (HIP) + solution annealing. The HIP is a thermal process in which high temperatures at the the isostatic pressure of one gas is applied to the material.
- **Treatment 3**: solution annealing + porous coating + HIP + solution annealing. The porous coating procedure is a thermal treatment employed in the manufacturing of surface prostheses. In this, spherical beads are bonded to each other and the solid substrate by sintering at high temperatures (1300ºC) to achieve a strong particle-particle substrate bond (Jacobbs et al, 1990).

The microstructure **1** reveals high amount of carbides in the matrix and in the grain boundaries after the solution annealing. The microstructure of the thermal treatment **2** presents greater homogeneity of the carbide precipitation than thermal treatment **1** (decrease in the number of carbides). This fact is due to the dissolution of carbides within the cobalt matrix as a consequence of more complex process in the thermal treatments. Finally, the microstructure **3** is characterized by an enhanced growth of the grain size and a diminution of the amount of carbides due to the porous coating process.

The Nyquist diagram represented in Fig. 11 was obtained at an applied passive potential. According to these diagrams the EEC used to model the experimental data is shown in Fig. 6(a). The impedance spectrum of the alloy strongly changes depending on the thermal treatment; R_{in} increases and CPE_{in} diminishes with the carbide solubilisation. In this case, the treatment **3** (which presents the highest grain size and the lowest amount of carbides) provides to the CoCrMo alloy the most protective layer under passive conditions (highest values of R_{in}) and the thickest passive film (lowest value of the CPE_{in}).

Thus impedance technique allows comparing the resistance of the passive dissolution of a CoCrMo alloy subjected to different thermal treatments and concluding that changing grain

size and carbide content in the alloy it is possible to improve the biocompatibility of the biomaterial.

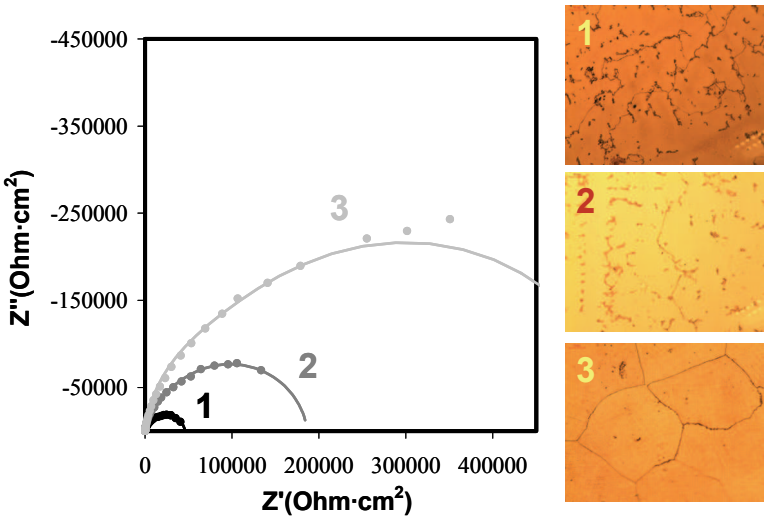

Fig. 11. Optical images of the microstructures of three different thermal treatments applied on an as-cast CoCrMo alloy and the Nyquist diagram of each sample at an applied passive potential in Bovine Serum solution (Valero & Igual, 2009).

5. Conclusions

Electrochemical Impedance Spectroscopy (EIS) has been demonstrated to be a sensitive and powerful tool for characterizing the interface and quantifying the metal release (biocompatibility) of biomedical alloys in simulated body fluids. In this chapter, the influence of material properties (chemical composition, grain size, and carbide content) and environmental factors (temperature, chemical composition of the simulated body fluids and adsorption of proteins) on the electrochemical behaviour of CoCrMo biomedical alloys has been studied by EIS.

The analysis of the impedance results allows the characterization and the quantification of different electrochemical and chemical process occurring on the biomaterial surface. It is possible to quantify the amount of adsorbed protein onto the surface and to calculate thermodynamic and kinetic parameters of the process (i.e. Gibbs free energy of adsorption, activation energy) by using the values of the charge transfer resistance with impedance measurements.

Corrosion mechanisms have been elucidated by EIS under well-established electrochemical conditions (potentiostatically controlled in order to work with specific surface chemistry): in the passive state the corrosion mechanisms of CoCrMo is governed by passive dissolution, while under cathodic conditions the mass transport limitation by diffusion takes place. At an applied transpassive potential the corrosion process is accompanied by an adsorption process (due to presence of proteins) attributed to the relaxation of the corrosion products on the electrode surface.

The most common procedure to interpret impedance data is to propose an Equivalent Electrical Circuit (EEC) which quantitatively provides information about the interface characteristics, its structure, passive film properties, corrosion mechanisms and reactions taking place on the interface electrolyte/oxide passive film. But the possibility to use different EEC to represent the same electrochemical system makes difficult to establish a real model of the system. This uncertainty can be solved by a previous knowledge of the system (physical and electrochemical properties) and the use of Surface Analysis techniques as complementary tools to the electrochemical measurements. X-Photoelectron Spectroscopy (XPS) and Auger Electron Spectroscopy (AES) are examples of complementary techniques used to complete the information obtained by EIS measurements (composition of the passive film and oxidation state of the constituent elements). The accurate knowledge of the surface chemistry is an essential aspect for the fundamental understanding of the electrochemical processes occurring on the interface biomaterial/body fluid.
On the other hand, several experimental aspects must be considered for the analysis of the EIS results. The technique is limited by the steady-state conditions needed for the impedance measurements which is difficult to assure when working with biological systems (dynamic systems). Metallic implants are commonly subjected to mechanical loads and relative movements (non-steady conditions). Thus, further development of EIS technique should be done in order to characterize the metal behaviour under mechanical-electrochemical phenomena such as those found in tribocorrosion situations.

6. References

Bi, Q.; Liu, W.; Ma, J.; Yang, J. ; Pu, Y. & Xue, Q. (2009). Tribocorrosion bevavior of Ni-17.5Si-29.3Cr alloy in sulfuric acid solution. *Tribology International, 42*, 7, (July 2009) (1080-1087), ISSN 0301-679X.

Black, J. & Hastings G. (1998). *Handbook of biomaterial properties (Blood and related fluids)*, Chapman & Hall, ISBN 0-412-60330-6, London, United Kingdom.

Catelas, I.; Petit, A.; Zukor, D.J. & Huk, O.L. (2001). Cytotoxic and apoptotic effects of cobalt and chromium ions on J774 macrophages- Implication of caspase-3 in the apoptotic pathway. *Journal of Materials Science: Materials in Medicine, 12*, 10-12, (December 2001) (949-953), ISSN 0957-4530.

Dumbleton, J.M. & Manley J.M. (2005). Metal-on-metal total hip replacement: What does the literature say?. The Journal of Arthroplasty, 20, 2, (February 2005) (174-188), ISSN 0883-5403.

Ebied, A. & Journeaux, S. (2002). Mini-symposium: hip replacement. (iv) Metal-on-metal hip resurfacing. *Current Orthopaedics, 16*, 6, (December 2002) (420-425), ISSN 0268-0890.

Fleury C.; Petit A.; Mwale F.; Antoniuou J.; Zukor D.J.; Tabrizian M. & Huk O.L. (2006). Effect of cobalt and chromium ions on human MG-63 osteoblasts in vitro: Morphology, cytotoxicity, and oxidative stress. *Biomaterials, 27*, 18, (June 2006) (3351-3360), ISSN 0142-9612.

Germain, M.A.; Hatton A.; Williams S.; Matthews J.B.; Stone M.H.; Fisher J. & Ingham E. (2003). Comparison of the cytotoxicity os clinically relevant cobalt-chromium and alumina ceramic wear particles in vitro. *Biomaterials, 24*, 3, (February 2003) (469-479), ISSN 0142-9612.

Granchi, D.; Cenni, E.; Trisolino, G.; Giunti, A. & Baldini N. (2006). Sensitivity to implant materials in patients undergoing total hip replacement. *Journal of Biomedical*

Materials Research. Part B: Applied Biomaterials, 77, 2, (May 2006) (257-264), ISSN 1552-4973.

Hallab, N.J.; Mikecz, K. & Jacobs J.J. (2000). A triple assay technique for the evaluation of metal-induced, delayed-type hypersensitivity responses in patients with or receiving total joint arthroplasty. *Journal of Biomedical Materials Research, 53*, 5, (September 2000) (480-489), ISSN 0021-9304.

Hallab, N.J.; Mikecz, K.; Vermes, C.; Skipor, A. & Jacobs, J.J. (2001) Orthopaedic implant related metal toxicity in terms of human lymphocyte reactivity to metal-protein complexes produced from cobalt-base and titanium-base implant alloy degradation. *Molecular and Cellular Biochemistry, 222*, 1-2, (June 2001) (127-136) ISSN 0300-8177.

Hanawa (2001). Characterization of the surface oxide film of a Co–Cr–Mo alloy after being located in quasi-biological environments using XPS. Applied Surface Science, 183, 1-2, (November 2001) (68-75), ISSN 0169-4332.

Hanawa, T. (2004). Metal ion release from metal implants. *Materials Science and Engineering C, 24*, 6-8, (December 2004) (745-752), ISSN 0928-4931.

Helsen J.A. & Breme H.J. (1998). *Metals as biomaterials,* John Wiley & Sons Ltd, ISBN 0-471-96935-4, United Kingdom.

Hodgson, A.W.E; Kurz, S.; Virtanen, S.; Fervel, V.; Olsson, C.-O.A. & Mischler, S. (2004). Passive and tranpassive behaviour of CoCrMo in simulated biological solutions. *Electrochimica Acta, 49*, 13, (May 2004) (2167-2178), ISSN 0013-4686.

Horowitz, S.M; Luchetti, W.T.; Gonzales, J.B. & Ritchie, C.K. (1998). The effect of cobalt chromium upon macrophages. *Journal of Biomedical Materials Research, 41*, 3, (September 1998) (468-473), ISSN 0021-9304.

Igual Muñoz, A. & Mischler, S. (2007). Interactive effects of albumin and phosphates ions on the corrosion of CoCrMo implant alloy. *Journal of the Electrochemical Society, 154*, 10, (August 2007) (C562-C570), ISSN 0013-4651.

Igual Muñoz, A. & Casabán Julián, L. (2010). Influence of electrochemical potential on the tribocorrosion behaviour of high carbon CoCrMo biomedical alloy in simulated body fluids by electrochemical impedance spectroscopy. *Electrochimica Acta, 55*, 19, (30 July 2010) (5428-5439), ISSN 0013-4686.

Jacobs, J.J.; Latanision, R.M.; Rose R.M. & Veeck, S.J. (1990). The effect of porous coating processing on the corrosion behavior of cast Co-Cr-Mo surgical implant alloys. *Journal of Orthopaedic Research, 8*, 6, (November 1990) (874-882), ISSN 0736-0266.

Kanagaraja, S.; Lundström, I.; Nygren, H.; Tengvall, P. Platelet binding and protein adsorption to titanium and gold after short time exposure to heparinized plasma and whole blood. *Biomaterials, 17*, 23, (1996) (2225-2232), ISSN 0142-9612.

Khan, M.A.; Williams, R.L. & Williams D.F. (1996). In-vitro corrosion and wear of titanium alloys in the biological environment. *Biomaterials, 17*, 22, (November 1996) (2117-2126), ISSN 0142-9612

Kocijan, A.; Milosev, I.; Merl, D.K. & Pihlar B. (2004). Electrochemical study of Co-based alloys in simulated physiological solution. *Journal of Applied Electrochemistry, 34*, 5, (May 2004) (517-524), ISSN 0021-891X.

Landolt, D. (2007). *Corrosion and surface chemistry of metals,* EPFL Press, ISBN 978-2-940222-11-7, Lausanne, Switzerland.

Marcus, P. & Oudar, J. (1995). *Corrosion mechanisms in theory and practice,* Marcel Dekker, ISBN 0-8247-9592-X, New York, Unites States of America.

Massè A.; Bosetti, M.; Buratti, C.; Visentin, O.; Bergadano, D. & Cannas M. (2003). Ion release and chromosomal damage from total hip prostheses with metal-on-metal articulation. *Journal of Biomedical Materials Research. Part B: Applied Biomaterials, 67*, 2, (November 2003) (750-757), ISSN 1552-4973.

Metikos-Hukovic, M.; Pilic, Z.; Babic, R. & Omanovic, D. (2006). Influence of alloying elements on the corrosion stability of CoCrMo implant alloy in Hank's solution. *Acta Biomaterialia*, 2, 6, (November 2006) (693-700), ISSN 1742-7061.

Metikos-Hukovic, M. & Babic, R. (2007). Passivation and corrosion behaviours of cobalt and cobalt-chromium-molybdenum alloy. *Corrosion Science*, *49*, 9, (September 2007) (3570-3579), ISSN 0010-938X.

Militello, V.; Vetri V. & Leone, M. (2003). Conformational changes involved in thermal aggregation processes of bovine serum albumin. *Biophysical Chemistry, 105*, 1, (August 2003) (133-141), ISSN 0301-4622.

Milosev, I. & Strehblow, H.-H. (2003). The composition of the surface passive film formed on CoCrMo alloy in simulated physiological solution. *Electrochimica Acta, 48*, 19, (August 2003) (2767-2774), ISSN 0013-4686.

Okazaki Y. & Gotoh E. (2005). Comparison of metal release from various metallic biomaterials in vitro. *Biomaterials, 26*, 1, (January 2005) (11-21), ISSN 0142-9612.

Ouerd, A.; Alemany-Dumont, C.; Normand, B. & Szunerits, S. (2008). Reactivity of CoCrMo alloy in physiological medium: Electrochemical characterization of the metal/protein interface. *Electrochimica Acta, 53*, 13, (May 2008) (4461-4469), ISSN 0013-4686.

Scully J.R.; Silverman D.C. & Kending M.W. (1993). *Electrochemical impedance. Analysis and interpretation,* American Society for testing and materials (ASTM), ISBN 0-8031-1861-9, Philadelphia, United States of America.

Szklarska-Smialowska, Z. (1986). *Pitting corrosion of metals*, National Association of Corrosion Engineers (NACE) publications, ISBN 0-915567-19-9, Houston, Texas, United States of America.

Tipper, J.L; Ingham, E.; Jin, Z.M. & Fisher, J. (2005). Mini-symposium: hip replacement. (iv) The science of metal-on-metal articulation. *Current Orthopaedics, 19*, 4, (August 2005) (280-287), ISSN 0268-0890.

Valero Vidal, C. & Igual Muñoz, A. (2008). Electrochemical characterisation of biomedical alloys for surgical implants in simulated body fluids. *Corrosion Science, 50*, 7, (July 2008) (1954-1961), ISSN 0010-938X.

Valero Vidal, C. & Igual Muñoz, A. (2009). Effect of termal treatment and applied potencial on the electrochemical behaviour of CoCrMo biomedical alloy. *Electrochimica Acta, 54*, 6, (February 2009) (1789-1809), ISSN 0013-4686.

Valero Vidal, C.; Olmo Juan, A. & Igual Muñoz, A. (2010). Adsorption of bovine serum albumin on CoCrMo surface: effect of temperature and protein concentration. *Colloids and Surfaces B: Biointerfaces, 80*, 1, (October 2010) (1-10), ISSN 0927-7765.

Valero Vidal, C.; Mischler S.; Olsson, C.-O.A. & Igual Muñoz A. (2010). Passive behaviour of a CoCrMo biomedical alloy studied by EQCM and XPS, *Proceedings of 51st Corrosion Science Symposium*, Abstract 27, September 2010, Southampton.

Virtanen S.; Milosev, I.; Gomez-Barrena, E.; Trebse, R.; Salo, J. & Konttinen Y.T. (2008). Special modes of corrosion under physiological and simulated physiological conditions. *Acta Biomaterialia, 4*, 3, (May 2008) (468-476), ISSN 1742-7061.

Wolner, C.; Nauer, G.E.; Trummer, J.; Putz, V. & Tschegg, S. (2006). Possible reasons for the unexpected bad biocompatibility of metal-on-metal hip implants. *Materials Science and Engineering C, 26*, 1, (January 2006) (34-40), ISSN 0928-4931.

Biomedical Engineering, Trends in Materials Science
Edited by Mr Anthony Laskovski

ISBN 978-953-307-513-6
Hard cover, 564 pages
Publisher InTech
Published online 08, January, 2011
Published in print edition January, 2011

Rapid technological developments in the last century have brought the field of biomedical engineering into a totally new realm. Breakthroughs in materials science, imaging, electronics and, more recently, the information age have improved our understanding of the human body. As a result, the field of biomedical engineering is thriving, with innovations that aim to improve the quality and reduce the cost of medical care. This book is the second in a series of three that will present recent trends in biomedical engineering, with a particular focus on materials science in biomedical engineering, including developments in alloys, nanomaterials and polymer technologies.

InTech Europe
University Campus STeP Ri
Slavka Krautzeka 83/A
51000 Rijeka, Croatia
Phone: +385 (51) 770 447
Fax: +385 (51) 686 166
www.intechopen.com

InTech China
Unit 405, Office Block, Hotel Equatorial Shanghai
No.65, Yan An Road (West), Shanghai, 200040, China
中国上海市延安西路65号上海国际贵都大饭店办公楼405单元
Phone: +86-21-62489820
Fax: +86-21-62489821